PHYSICAL REVIEW A **101**, 032510 (2020)

Capturing multireference excited states by constrained-density-functional theory

Nell Karpinski,[1] Pablo Ramos,[1,*] and Michele Pavanello[1,2,†]
[1]*Department of Chemistry, Rutgers University, Newark, New Jersey 07102, USA*
[2]*Department of Physics, Rutgers University, Newark, New Jersey 07102, USA*

(Received 4 November 2019; accepted 26 February 2020; published 23 March 2020)

The computation of excited electronic states with commonly employed (approximate) methods is challenging, typically yielding states of lower quality than the corresponding ground state for a higher computational cost. In this work, we present a mean-field method that extends the previously proposed excited constrained-density-functional theory (XCDFT) from single Slater determinants to ensemble one-body reduced density matrices for computing low-lying excited states. The method still retains an associated computational complexity comparable to a semilocal density functional theory (DFT) calculation while at the same time it is capable of approaching states with multireference character. We benchmark the quality of this method on well-established test sets, finding good descriptions of the electronic structure of multireference states and maintaining an overall accuracy for the predicted excitation energies comparable to semilocal time-dependent DFT.

DOI: 10.1103/PhysRevA.101.032510

I. INTRODUCTION

Models of molecules and materials typically require the knowledge of excited electronic states and must be able to approach complex dynamical regimes. For example, in energy sciences and photochemistry, often the dynamics involve interaction with external electromagnetic fields or require characterization of states that are very close in energy. Thus, the task at hand is formulating a computationally efficient model of electronic excited states capable of handling the many difficult cases that, unfortunately, routinely arise.

Density functional theory (DFT) has been the workhorse of electronic structure theory for the computation of excited electronic states and their dynamics via its time-dependent extension (TDDFT). Unfortunately, TDDFT has some notable shortcomings when it is implemented in the adiabatic and the semilocal density approximations. Conical intersections, charge transfer states, and Rydberg states are among those cases where practical implementations of TDDFT struggle to provide a physical model. More recently, multiconfigurational DFT methods, such as ensemble DFT [1–5], constrained DFT [6–8], block-localized DFT [9,10], DFT/MRCI (multireference configuration interaction) [11], and even flavors of ground-state DFT [12] have been proposed as innovative protocols for extracting excitation energies in a computationally efficient way while still making use of density functionals in their formulation.

Constrained DFT [13] is particularly interesting because it does not need an active space and, instead, targets directly the excited states with the wanted character [14]. Traditionally it has been employed for generating charge and spin-localized states (diabatic states). However, recent works including our own have borrowed the general constrained DFT idea and proposed methods for computing valence excited states [6,7,15–17].

In this work, we continue the development of the excited constrained DFT (XCDFT) method [7]. In XCDFT, a variational procedure produces excited-state energies and densities of similar quality to the ground-state ones for a similarly comparable computational cost. In essence, XCDFT exploits the machinery of ground-state Kohn-Sham DFT for the generation of excited states [18–20]. Inspired by density functional perturbation theory [21], XCDFT does not require the use of unoccupied bands (virtuals) as it resolves the space of virtuals by projection. The Fock operator is then augmented by a nonlocal and orbital-dependent constraining potential exerting a force on the electrons, leading to a self-consistent solution for the targeted excited state. XCDFT is similar in spirit to Delta self consistent field method (ΔSCF) without the inconvenience of incurring in variational collapses. In our previous publication [7], we carried out a careful comparison of XCDFT against ΔSCF, and linear-response semilocal TDDFT and found that its accuracy compares to them (about 0.5–1.0 eV deviation from benchmark values for the chosen test set).

Unfortunately and similar to ΔSCF, due to the fact that XCDFT makes use of a single Slater determinant, when approaching degenerate excited states it fails to produce correct electronic structures. This is problematic because degenerate electronic excited states are ubiquitous.

In this work, we take inspiration from ensemble DFT methods and propose the use of ensemble one-body reduced density matrices (1-RDMs) for describing the electronic structure of excited states. We dub the resulting method τXCDFT. This allows us to partially occupy an excited state's Kohn-Sham (KS) orbitals and reach an accurate depiction of a multireference excited state at merely the expense of needing to compute a larger number of occupied orbitals.

The paper is organized as follows: We first describe the theory and implementation of τXCDFT and clearly show

---

[*] p.ramos@rutgers.edu

[†] m.pavanello@rutgers.edu

the involved approximations. After a short description of the computational details, needed for the reproducibility of the results, we apply τXCDFT on the same test set considered previously [7], as well as additional complex large molecules, such as anthracene, tetracene, and fullerene. These are included because the description of their excited states' electronic structure may require more than single excitations from the reference determinant. Due to the variational nature of τXCDFT, the orbitals are relaxed to infinite order, making up for the relaxation effects that are captured by multiple excitations in those wavefunction-based methods exploiting a reference determinant.

II. THEORY AND BACKGROUND

The starting point of an XCDFT calculation is a reference ground state (gs) obtained from a regular KS calculation. From that, a projection operator $\hat{P}_o^g$ over the occupied space of the gs, $\{|i_g\rangle\}$, is constructed, namely,

$$\hat{P}_o^g = \sum_{i_g=1}^{\text{occ}} |i_g\rangle\langle i_g|. \tag{1}$$

The electronic excitations are obtained by applying a nonlocal potential, $\hat{W}_c$, whose action is to "fish out" a custom number of electrons (i.e., N_c, which we take to be $N_c = 1$ throughout this work) into the virtual space of the reference gs. In the basis of the atomic orbitals (customarily indicated by Greek letters, ν and μ), such potential is written as

$$(\hat{W}_c)_{\mu\nu} = \langle \mu | \hat{1} - \hat{P}_o^g | \nu \rangle, \tag{2}$$

which then is used to define the constraint that only N_c electrons should be excited to the virtual space of the reference gs,

$$N_c = \sum_{j=1}^{\text{occ}} \langle j_e | \hat{1} - \hat{P}_o^g | j_e \rangle \equiv \text{Tr}[\hat{W}_c \hat{\gamma}_e]$$

$$= N_e - \sum_{i_g, j_e=1}^{\text{occ}} \langle j_e | i_g \rangle \langle i_g | j_e \rangle. \tag{3}$$

Here $\hat{\gamma}_e$ is the 1-RDM of the excited state, N_e is the total number of electrons, N_c is the number of excited electrons (which is typically taken to be $N_c = 1$), and $|j_e\rangle$ are the excited-state occupied orbitals which are self-consistently determined by the following KS-like equation:

$$\left[-\tfrac{1}{2}\nabla^2 + v_s(\mathbf{r}) + V_c \hat{W}_c\right] |j_e\rangle = \varepsilon_{j_e} |j_e\rangle, \tag{4}$$

where $v_s(\mathbf{r})$ is the Kohn-Sham potential, ε_{j_e} are the orbital energies, and V_c is an appropriate Lagrange multiplier that ensures the constraint Eq. (3) is satisfied. In other words,

$$\frac{\delta E[\hat{\gamma}_e]}{\delta N_c} = -V_c, \tag{5}$$

where $E[\hat{\gamma}_e]$ is the total energy functional [7,22]. In this context, V_c equals the value of the excitation energy (i.e., the work needed to excite one electron) and needs to be determined self-consistently.

XCDFT yields excitation energies in semiquantitative agreement with TDDFT and benchmark calculations; however, we noticed [7] that whenever it is required to go beyond a single Slater determinant, spurious contributions from more than singly excited configuration state functions arise, degrading the excited state's electronic structure. One particularly deteriorating factor is the resulting significant overlap with the gs KS wavefunction. As this problem only arises when multireference excited states are considered, we turned to the several studies carried out to understand and deal with static correlation in Kohn-Sham DFT [23–25]. It is known that when near degeneracies arise (typical case of a multireference system), an ensemble of noninteracting electrons provides a more convenient reference than typical single Slater determinants [24,26]. Thus, in this work, we allow XCDFT excited states to probe ensemble 1-RDMs as follows:

$$\hat{\gamma}_e = \sum_{j_e} |j_e\rangle f_{j_e} \langle j_e|, \tag{6}$$

with f_{j_e} the occupation numbers which are determined by the Fermi-Dirac distribution function,

$$f_{j_e} \equiv f(\varepsilon_{j_e} - \mu) = \left[1 + \exp\left(\beta\left(\varepsilon_{j_e} - \mu\right)\right)\right]^{-1}, \tag{7}$$

with $\beta = \frac{1}{k_B \tau}$ (a parameter of the method), and μ can be thought of as a chemical potential. Smearing the orbital occupations is a well-known strategy that has been used in mean-field calculations [27] of both finite and periodic systems when degeneracies appear.

Thus, Eq. (3) is modified to

$$N_c = \text{Tr}[\hat{W}_c \hat{\gamma}_e] = N_e - \sum_{i_g}^{occ} \sum_{j_e}^{\infty} \langle i_g | j_e \rangle f_{j_e} \langle j_e | i_g \rangle. \tag{8}$$

We dub the resulting method τXCDFT.

III. COMPUTATIONAL DETAILS

All XCDFT and τXCDFT excited-state calculations are performed with a development version of the Amsterdam Density Functional (ADF) 2019 program [28]. To assess the performance of τXCDFT, we consider the lowest excited state for a set of 15 molecules [7] with the addition of anthracene, tetracene, and fullerene. As described above (see Theory section), we rely on the approximation that smearing provided by the Fermi-Dirac distribution function is sufficient to account for the fractional occupations resulting from the multireference character of certain excited states. This smearing can be achieved by employing a Fermi-Dirac distribution with $\tau = 500$ K which is consistently applied to all systems considered. The chemical potential, μ, is obtained by imposing that the number of electrons be equal to N_e through finding the root by bisection of the function $h(\mu) = N(\mu) - N_e$. After some testing, the numerical convergence of this root-finding algorithm could not be achieved for τ values much lower than 500 K. Therefore, $\tau = 500$ K is a choice that avoids unwanted occupations of high-lying virtual orbitals while delivering a stable algorithm. The generalized gradient approximation (GGA) Perdew-Burke-Ernzerhof (PBE) functional [29] and the meta-GGA functionals M06-L [30], strongly constrained and appropriately normed semilocal density functional (SCAN) [31] and revised Tao-Perdew-Staroverov-Scuseria functional (revTPSS) [32] are employed

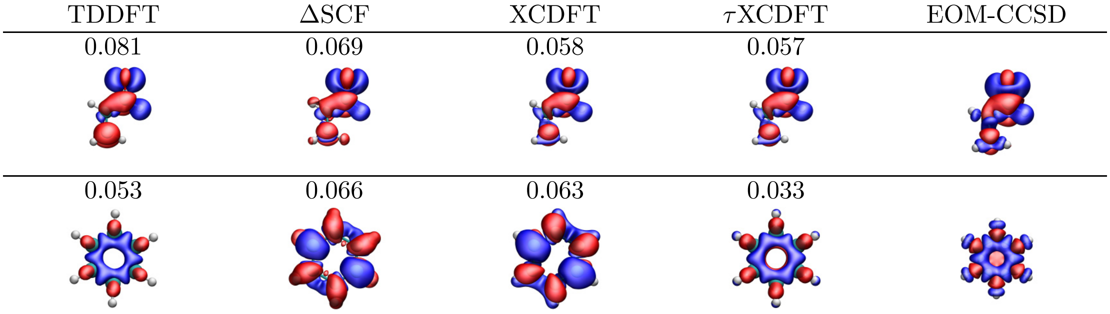

FIG. 1. Comparison of the computed differential densities for acrolein (top) and benzene (bottom). We show all DFT functionals used against EOM-CCSD. The standard deviation, σ, of each density difference against EOM-CCSD densities (calculated using Gaussian [34]) is shown.

across the entire study along with the Triple-zeta basis sets. We report XCDFT and τXCDFT excitation energies by using the value of the corresponding V_c Lagrange multiplier. In addition, the differential densities obtained with XCDFT are compared against the ones obtained from TDDFT, calculated with ORCA [33].

IV. RESULTS AND DISCUSSION

A. Quality of the electron density

We carried out an analysis of the electronic densities by comparing the differential densities [i.e., the density difference between the excited-state and ground-state densities, $\Delta(\mathbf{r}) = \rho_e(\mathbf{r}) - \rho_g(\mathbf{r})$] obtained form τXCDFT, XCDFT, TDDFT, and equation-of-motion coupled-cluster singles and doubles (EOM-CCSD). In Fig. 1, $\Delta(\mathbf{r})$ is displayed for acrolein and benzene.

EOM-CCSD is accurate for these systems, as both single and double excitations are accounted for in the method. In Fig. 1, we can see that the τXCDFT densities are improved with respect to the other methods. In our previous work [7], we showed that XCDFT densities (especially for benzene) are as inaccurate as the ones computed with ΔSCF and the results of Fig. 2 confirm this observation also for other molecules featuring exact degeneracy (such as fullerene). We notice that τXCDFT is able to capture more accurately the electron density of the excited states compared to the original XCDFT. TDDFT is overall in good agreement with the benchmark; however, it lacks some small features. For example, the negative equatorial component in the EOM-CCSD density of benzene is partially present in τXCDFT but absent in TDDFT (as we could verify by inflating the isosurfaces and double checking the cube files). Such nodal structure in the differential densities is commonly found in the literature and is expected when substantial orbital relaxation occurs. Accounting for orbital relaxation in linear-response TDDFT has been a matter of intense study. For example, Ziegler *et al.*'s work on constricted variational TDDFT [15–17,35] aimed at capturing orbital relaxation via a variational energy minimization with respect to orbital rotations.

For acrolein, there are no degeneracies and thus τXCDFT and XCDFT deliver the same result which compares well against EOM-CCSD.

The orbital relaxation is also seen in fullerene (see Fig. 2), where the τXCDFT differential density follows the TDDFT one but is more delocalized, indicating relaxation. Unfortunately, due to the large computational expense involved, we do not have an EOM-CCSD calculation available to further confirm our findings.

From the above analysis, it is clear that the restriction in XCDFT and ΔSCF to a single Slater determinant is detrimental to the quality of the electronic structure of multireference excited states. In particular, focusing on the benzene molecule, we notice that in order to satisfy the criterion of excitation of a single electron, XCDFT's excited-state orbitals are mixed (e and g superscripts indicate excited and ground states, respectively):

$$\phi_H^e(\mathbf{r}) = \frac{1}{\sqrt{2}}\left[\phi_H^g + \phi_{L+1}^g\right], \tag{9}$$

$$\phi_{H-1}^e(\mathbf{r}) = \frac{1}{\sqrt{2}}\left[\phi_{H-1}^g + \phi_L^g\right]. \tag{10}$$

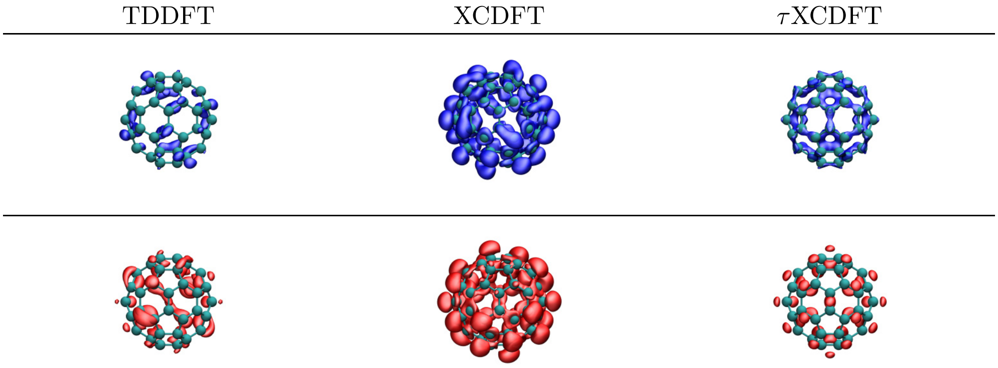

FIG. 2. Fullerene density differences divided by contribution $\Delta(\mathbf{r}) > 0$ in blue (top) and $\Delta(\mathbf{r}) < 0$ in red (bottom). All isosurfaces are plotted with the same cutoff.

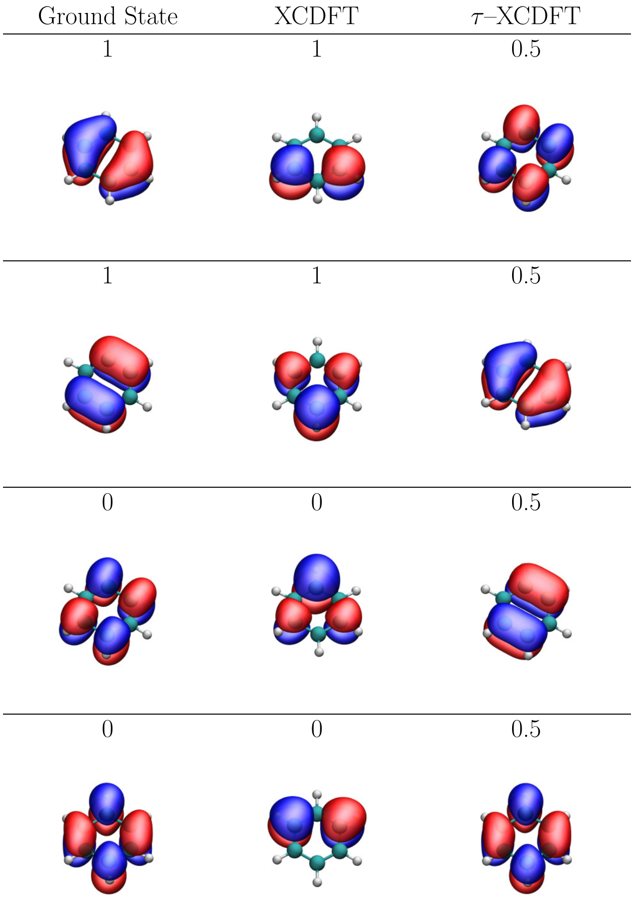

FIG. 3. Comparison of the frontier molecular orbitals of benzene obtained with τXCDFT and XCDFT against the corresponding ground-state orbitals. The occupation numbers of these orbitals are shown.

TABLE I. τXCDFT excitation energy values (in eV) for all exchange-correlation functionals considered. The excitation energies of systems with excited states of mixed character as seen in Fig. S2 [42] are denoted in bold font.

System	PBE	M06-L	SCAN	revTPSS	Benchmark
Ethylene	6.06	6.14	5.90	6.08	7.80
Tetrafluoroethylene	6.23	6.59	6.42	6.35	7.08
Isoprene	4.99	4.53	4.35	5.32	5.74
1,3-butadiene	4.56	4.51	4.35	4.56	6.18
Formaldehyde	3.95	3.48	2.86	3.48	3.88
Propanamide	5.76	5.51	5.11	5.79	5.72
Acrolein	3.89	3.28	2.68	3.42	3.75
Pyrrole	**5.46**	**5.73**	**5.52**	**5.57**	6.37
Thiophene	5.28	5.30	5.03	5.13	5.64
Benzaldehyde	3.75	3.31	2.67	3.49	3.34
Adenine	4.55	4.68	4.46	4.66	5.25
Cytosine	4.31	4.87	4.67	4.61	4.66
Benzene	**5.19**	**5.47**	**5.37**	**5.36**	5.08
Naphthalene	4.01	3.94	3.77	3.97	4.24
Anthracene	3.12	3.04	2.89	3.06	3.55
Tetracene	2.14	2.03	1.90	2.06	2.95
Pentacene	1.96	1.87	1.73	1.88	2.30
Fullerene	**1.59**	**1.73**	**1.69**	**1.65**	1.75

As a result, the excited-state wavefunction can be represented by the following superposition of configuration state functions built from the reference ground state and associated excited Slater determinants, namely,

$$\Psi_e = \tfrac{1}{2}\Psi_g + \tfrac{1}{2}\Psi^{L}_{H-1} + \tfrac{1}{2}\Psi^{L+1}_{H} + \tfrac{1}{2}\Psi^{L,L+1}_{H-1,H}. \qquad (11)$$

The above clearly indicates that the XCDFT excited-state wavefunction, Ψ_e, has strong overlap with the ground-state wavefunction, Ψ_g, and an equally strong double excitation character arising from the $\Psi^{L,L+1}_{H-1,H}$ term.

In our trial calculations (not reported), we have noticed that the above-described issue is shared among aromatic chromophores, casting serious doubts about the physicality of ΔSCF excited states which are frequently used as initial conditions for nonadiabatic dynamics simulations.

In Fig. 3, we plot the frontier occupied and virtual orbitals of the ground and XCDFT and τXCDFT excited states. The figure indicates that the τXCDFT orbitals largely resemble the ground-state orbitals with some small deviations due to orbital relaxation effects (typically accounted for in wavefunction methods by high-order excitation contributions). Instead, the XCDFT orbitals are very different from the ground-state ones, indicating that in XCDFT, in order to satisfy the imposed constraint in Eq. (3), the frontier orbitals have mixed and rotated dramatically, exposing an unphysical character. Thus, we can conclude this analysis by stating that, for multireference excited states, τXCDFT orbitals indicate a degree of relaxation compared to the ground-state orbitals while still retaining the overall character resulting in differential densities in agreement with EOM-CCSD calculations. A similar analysis can be carried out for fullerene, although it is not reported.

B. Quality of the excitation energies

We summarize in Table I the excitation energies computed with τXCDFT along with available benchmark data [36–41]. The performance of τXCDFT improves against XCDFT as the characters of the states involved are now corrected. We find that for multireference excited states (pyrrole, benzene, and fullerene) the energies are slightly closer to the benchmark. In addition, in Fig. S2 of the Supplemental Material [42], we show the electronic entropy computed for every excited state. By "electronic entropy" we refer to the electronic Gibbs entropy, which in this context can also be called Shannon entropy, $S = -\sum_i p_i \ln(p_i) + (1 - p_i)\ln(1 - p_i)$. Entropy in this context has no thermodynamical meaning; rather it has an information theory meaning. That is, it describes distributions (in this case distributions of occupation numbers) that are not infinitely narrow, but instead have a finite width. As expected, benzene and fullerene are those systems with the highest multireference character. In our previous work (Ref. [7]; see also Supplemental Material Table S2 [42]), we used a different descriptor for detecting multireference character. Specifically, we used the eigenvalues of the difference between the excited-state and the ground-state 1-RDMs which led us to label as "mixed" additional molecules to the ones mentioned here such as naphthalene, pentacene, and adenine.

TABLE II. Mean unsigned error against benchmark values across the entire set of all excitation energies computed for all exchange-correlation functionals and methods considered.

Method	PBE	M06-L	SCAN	revTPSS
XCDFT	0.677	0.447	0.378	0.503
τXCDFT	0.566	0.591	0.816	0.557
ΔSCF	1.320	0.790	1.660	1.420
TDDFT	0.390	0.620	0.513	0.375

These molecules still display a multireference excited state in the context of the present work; however, most likely the multireference character is captured already at the level of the orbital relaxation with no need to involve fractional orbital occupations. This explains why the entropy for these three systems is negligible, while the descriptor previously used flags them as multireference.

In principle τXCDFT should lead to higher-accuracy excitation energies than XCDFT for mixed excited states. In practice, however, both XCDFT and ΔSCF take advantage of error cancellation [7]. As we have seen in our previous work, while for highest occupied molecular orbital (HOMO)–lowest unoccupied molecular orbital (LUMO) excitations ΔSCF performs well [43], in the presence of a degenerate excited state, single-reference methods will result in HOMO-LUMO mixing [and mixing of lower- and higher-lying orbitals depending on the system; see Eqs. (9)–(11)]. This generates an excited-state Slater determinant that is a mix of ground, single excitations, and double excitations. The single excitations are associated with an accurate energy, the double excitations are associated with a much higher energy, and the ground-state contribution effectively hedges the double excitations. In our tests, τXCDFT never generates occupied-virtual mixed orbitals and delivers higher-quality electronic structures.

In Table II, we show the mean unsigned error (MUE) for the excitation energies computed with τXCDFT, XCDFT, ΔSCF, and TDDFT. The MUE shows that τXCDFT and XCDFT are comparable to TDDFT and significantly better than ΔSCF. We see that among all meta-GGA functionals, revTPSS is the better performing. In an effort to explain some of the trends, in Fig. 4 we report a histogram of a measure of spin contamination τXCDFT and XCDFT collecting all exchange-correlation functionals considered (i.e., overlap between the α and β orbitals). The histograms show that overall the spin contamination is well handled by XCDFT and τXCDFT. However, we notice that in τXCDFT the spin contamination is less prevalent, and we also note that the systems with high contamination (above 0.5) correspond to benzene and fullerene (i.e., where there are strong degeneracies among the frontier orbitals) computed with the SCAN functional.

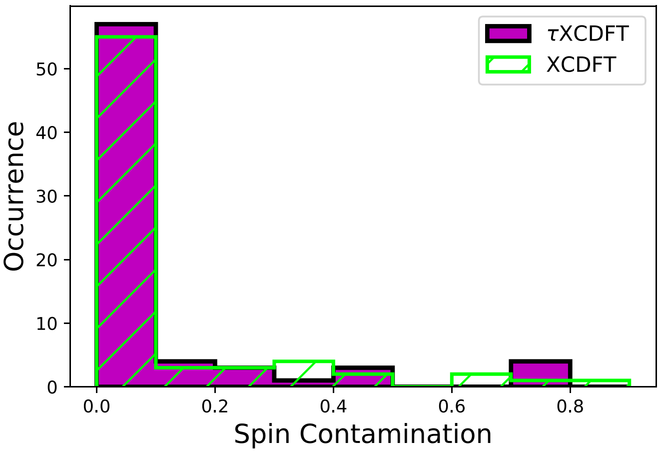

FIG. 4. Histogram of the spin contamination for all XCDFT and τXCDFT excited states collecting all exchange-correlation functionals.

For the sake of a complete presentation, we carry out an analysis of the sensitivity of the results with the chosen Fermi-Dirac smearing. We report our finding in Fig. S1 and Table S1 of the Supplemental Material [42]. Generally, τXCDFT energies improve if the KS gap is much smaller than the true gap of the interacting system. This points to a negative aspect of using unnecessarily broad smearing parameters ($\tau > 500$); i.e., the Fermi-Dirac distribution may populate high-lying virtual orbitals, which is not desired.

V. CONCLUSIONS

In conclusion, we developed, implemented in the ADF program, and benchmarked a mean-field method for the computation of low-lying electronic excited states, τXCDFT. This method is capable of accounting for degenerate energy levels often present in excited states, such as aromatic chromophores. We show that quality low-lying excited states are found by using ensemble 1-RDMs. We also show that when considering multireference excited states, mean-field methods that employ a single Slater determinant (such as ΔSCF and XCDFT) completely fail in predicting the electronic structure. τXCDFT instead reproduces the electronic density of these excited states, avoids incorrect rotation among the frontier orbitals, and correctly features effects of orbital relaxation.

ACKNOWLEDGMENTS

This material is based upon work supported by the U.S. Department of Energy, Office of Basic Energy Sciences, under Award No. DE-SC0018343. The authors acknowledge the Office of Advanced Research Computing (OARC) at Rutgers, The State University of New Jersey, for providing access to the Amarel cluster and associated research computing resources that have contributed to the results reported here.

[1] M. Filatov, WIREs: Comput. Mol. Sci. **5**, 146 (2014).
[2] M. Filatov, T. J. Martínez, and K. S. Kim, J. Chem. Phys. **147**, 064104 (2017).
[3] Z.-h. Yang, A. Pribram-Jones, K. Burke, and C. A. Ullrich, Phys. Rev. Lett. **119**, 033003 (2017).
[4] K. Deur and E. Fromager, J. Chem. Phys. **150**, 094106 (2019).

[5] O. Franck and E. Fromager, Mol. Phys. **112**, 1684 (2013).

[6] F. A. Evangelista, P. Shushkov, and J. C. Tully, J. Phys. Chem. A **117**, 7378 (2013).

[7] P. Ramos and M. Pavanello, J. Chem. Phys. **148**, 144103 (2018). [**152**, 109902 (2020)].

[8] B. Kaduk, T. Kowalczyk, and T. Van Voorhis, Chem. Rev. **112**, 321 (2012).

[9] A. Cembran, A. Payaka, Y. lin Lin, W. Xie, Y. Mo, L. Song, and J. Gao, J. Chem. Theory Comput. **6**, 2242 (2010).

[10] A. Cembran, L. Song, Y. Mo, and J. Gao, J. Chem. Theory Comput. **5**, 2702 (2009).

[11] S. Grimme and M. Waletzke, J. Chem. Phys. **111**, 5645 (1999).

[12] Y. Mei and W. Yang, J. Phys. Chem. Lett. **10**, 2538 (2019).

[13] T. Van Voorhis, T. Kowalczyk, B. Kaduk, L.-P. Wang, C.-L. Cheng, and Q. Wu, Annu. Rev. Phys. Chem. **61**, 149 (2010).

[14] Q. Wu and T. Van Voorhis, J. Chem. Phys. **125**, 164105 (2006).

[15] Y. C. Park, F. Senn, M. Krykunov, and T. Ziegler, J. Chem. Theory Comput. **12**, 5438 (2016).

[16] I. Seidu, M. Krykunov, and T. Ziegler, Mol. Phys. **112**, 661 (2014).

[17] T. Ziegler, M. Krykunov, and J. Cullen, J. Chem. Phys. **136**, 124107 (2012).

[18] P. W. Ayers and M. Levy, Phys. Rev. A **80**, 012508 (2009).

[19] P. W. Ayers, M. Levy, and A. Nagy, Phys. Rev. A **85**, 042518 (2012).

[20] M. Levy and Á. Nagy, Phys. Rev. Lett. **83**, 4361 (1999).

[21] S. Baroni, P. Giannozzi, and A. Testa, Phys. Rev. Lett. **58**, 1861 (1987).

[22] Q. Wu and T. Van Voorhis, Phys. Rev. A **72**, 024502 (2005).

[23] E. H. Lieb, Int. J. Quantum Chem. **24**, 243 (1983).

[24] P. R. T. Schipper, O. V. Gritsenko, and E. J. Baerends, Theor. Chem. Acc. **99**, 329 (1998).

[25] O. V. Gritsenko and E. J. Baerends, Theor. Chem. Acc. **96**, 44 (1997).

[26] S. G. Wang and W. H. E. Schwarz, J. Chem. Phys. **105**, 4641 (1996).

[27] J. C. Slater, J. B. Mann, T. M. Wilson, and J. H. Wood, Phys. Rev. **184**, 672 (1969).

[28] E. J. Baerends, T. Ziegler, A. J. Atkins, J. Autschbach, D. Bashford, O. Baseggio, A. Bérces, F. M. Bickelhaupt, C. Bo, P. M. Boerritger, L. Cavallo, C. Daul, D. P. Chong, D. V. Chulhai, L. Deng, R. M. Dickson, J. M. Dieterich, D. E. Ellis, M. van Faassen, A. Ghysels, A. Giammona, S. J. A. van Gisbergen, A. Goez, A. W. Götz, S. Gusarov, F. E. Harris, P. van den Hoek, Z. Hu, C. R. Jacob, H. Jacobsen, L. Jensen, L. Joubert, J. W. Kaminski, G. van Kessel, C. König, F. Kootstra, A. Kovalenko, M. Krykunov, E. van Lenthe, D. A. McCormack, A. Michalak, M. Mitoraj, S. M. Morton, J. Neugebauer, V. P. Nicu, L. Noodleman, V. P. Osinga, S. Patchkovskii, M. Pavanello, C. A. Peeples, P. H. T. Philipsen, D. Post, C. C. Pye, H. Ramanantoanina, P. Ramos, W. Ravenek, J. I. Rodríguez, P. Ros, R. Rüger, P. R. T. Schipper, D. Schlüns, H. van Schoot, G. Schreckenbach, J. S. Seldenthuis, M. Seth, J. G. Snijders, M. Solà, S. M., M. Swart, D. Swerhone, G. te Velde, V. Tognetti, P. Vernooijs, L. Versluis, L. Visscher, O. Visser, F. Wang, T. A. Wesolowski, E. M. van Wezenbeek, G. Wiesenekker, S. K. Wolff, T. K. Woo, and A. L. Yakovlev, ADF2019, SCM (Theoretical Chemistry, Vrije Universiteit, Amsterdam, 2019), https://www.scm.com.

[29] J. P. Perdew, K. Burke, and M. Ernzerhof, Phys. Rev. Lett. **77**, 3865 (1996).

[30] Y. Zhao and D. G. Truhlar, Theor. Chem. Acc. **120**, 215 (2008).

[31] J. Sun, A. Ruzsinszky, and J. P. Perdew, Phys. Rev. Lett. **115**, 036402 (2015).

[32] J. P. Perdew, A. Ruzsinszky, G. I. Csonka, L. A. Constantin, and J. Sun, Phys. Rev. Lett. **103**, 026403 (2009).

[33] F. Neese, WIREs: Comput. Mol. Sci. **2**, 73 (2012).

[34] M. J. Frisch, G. W. Trucks, H. B. Schlegel, G. E. Scuseria, M. A. Robb, J. R. Cheeseman, G. Scalmani, V. Barone, G. A. Petersson, H. Nakatsuji, X. Li, M. Caricato, A. V. Marenich, J. Bloino, B. G. Janesko, R. Gomperts, B. Mennucci, H. P. Hratchian, J. V. Ortiz, A. F. Izmaylov, J. L. Sonnenberg, D. Williams-Young, F. Ding, F. Lipparini, F. Egidi, J. Goings, B. Peng, A. Petrone, T. Henderson, D. Ranasinghe, V. G. Zakrzewski, J. Gao, N. Rega, G. Zheng, W. Liang, M. Hada, M. Ehara, K. Toyota, R. Fukuda, J. Hasegawa, M. Ishida, T. Nakajima, Y. Honda, O. Kitao, H. Nakai, T. Vreven, K. Throssell, J. A. Montgomery, Jr., J. E. Peralta, F. Ogliaro, M. J. Bearpark, J. J. Heyd, E. N. Brothers, K. N. Kudin, V. N. Staroverov, T. A. Keith, R. Kobayashi, J. Normand, K. Raghavachari, A. P. Rendell, J. C. Burant, S. S. Iyengar, J. Tomasi, M. Cossi, J. M. Millam, M. Klene, C. Adamo, R. Cammi, J. W. Ochterski, R. L. Martin, K. Morokuma, O. Farkas, J. B. Foresman, and D. J. Fox, GAUSSIAN 16 Revision C.01 (gaussian Inc., Wallingford, CT, 2016).

[35] J. Cullen, M. Krykunov, and T. Ziegler, Chem. Phys. **391**, 11 (2011).

[36] M. Schreiber, M. R. Silva-Junior, S. P. A. Sauer, and W. Thiel, J. Chem. Phys. **128**, 134110 (2008).

[37] M. R. Silva-Junior, M. Schreiber, S. P. A. Sauer, and W. Thiel, J. Chem. Phys. **129**, 104103 (2008).

[38] G. Martins, A. M. Ferreira-Rodrigues, F. N. Rodrigues, G. G. B. de Souza, N. J. Mason, S. Eden, D. Duflot, J.-P. Flament, S. V. Hoffmann, J. Delwiche, M.-J. Hubin-Franskin, and P. Limao-Vieira, Phys. Chem. Chem. Phys. **11**, 11219 (2009).

[39] D. M. P. Holland, A. B. Trofimov, E. A. Seddon, E. V. Gromov, T. Korona, N. de Oliveira, L. E. Archer, D. Joyeux, and L. Nahon, Phys. Chem. Chem. Phys. **16**, 21629 (2014).

[40] F. M. Floris, C. Filippi, and C. Amovilli, J. Chem. Phys. **140**, 034109 (2014).

[41] P. M. Zimmerman, Z. Zhang, and C. B. Musgrave, Nat. Chem. **2**, 648 (2010).

[42] See Supplemental Material at http://link.aps.org/supplemental/10.1103/PhysRevA.101.032510 for Additional tables and figures showing the dependency of the excitation energies with respect to τ, also we show evidence of multireference character by computing the electronic entropy and ground-excited state overlap for all systems considered.

[43] T. Kowalczyk, S. R. Yost, and T. V. Voorhis, J. Chem. Phys. **134**, 054128 (2011).